—**Original**—

Assessment of Abdominal Aortic Aneurysms Using A Cone-beam CT System: An Experimental Phantom Study and an Initial Clinical Evaluation Before and After Stent-graft Treatment in Patients with an Abdominal Aortic Aneurysm

Kazuo Ichikawa[1], Tatsuo Kumazaki[1], Hiromitsu Hayashi[1] and Masami Ochi[2]

[1]Department of Radiology, Center for Advanced Medical Technology and
[2] Second Department of Surgery, Nippon Medical School

Abstract

The aim of this study is to conduct a quantitative analysis of cone-beam CT (CBCT) images using a phantom, and then to evaluate the clinical usefulness of CBCT in the assessment of abdominal aortic aneurysms (AAA) before and after stent-grafting, both qualitatively as well as quantitatively. The phantom used in this study was a rectangular plate made of an acrylic resin, which contained eight through-holes to mimic blood vessels. Each columnar cavity was filled with contrast media and the diameter of each was then measured using a cone-beam multiplanar reformation/curved planar reformation (CB-MPR/CPR) technique, and the results were compared with the corresponding results obtained by actual measurement. In the clinical assessment, nine patients with AAA (consisting only of males with an average age of 68 years old: 56 ~80) were enrolled. The clinical qualitative analysis of CBCT consisted of: 1) for the pre-operative state, the shape of the aortic aneurysm, the relationship between the aneurysm and the aortic branches, and 2) for the post-operative state, the shape of the stent and any endoleakage present. The clinical quantitative analysis of CBCT included, for the aneurysm, its inflection angle, its maximum diameter, the diameter of the proximal and distal necks, and the distance of these two necks from specific reference points. The quantitative analysis using the phantom showed no significant differences between the results based on CB-MPR/CPR and those obtained by actual measurement. In the clinical qualitative analysis three-dimensional CBCT (3D-CBCT) depicted the anatomical relationship between the aneurysm and the aortic branches well, an accomplishment that was not possible by conventional angiography. Cone-beam maximum intensity projection (CB-MIP) was as good in tracing the migration and deformation of the stent following endovascular intervention as plain radiograms and conventional angiograms. CB-MPR/CPR enabled us to obtain any cross-sectional image of the aorta desired, including a curved, longitudinal cross-section of the aorta. Thus, with the CB-MPR/CPR technique it is easy to determine the distance of the proximal and distal necks of the aneurysm, and the inflection angle, and those results were not significantly different from those obtained by angiography. The diameter of the aneurysm, and the diameter of the proximal and distal necks as measured by CB-MPR/CPR images were significantly different from those obtained by conventional contrast

Correspondence to Kazuo Ichikawa, Department for Advanced Medical Technology, 1–1–5 Sendagi, Bunkyo-ku, Tokyo 113–8603, Japan
E-mail: rudolf@nms.ac.jp
Journal Website (http://www.nms.ac.jp/jnms/)

enhanced-CT (p<0.05). This suggests that CB-MPR/CPR yields a cross-sectional view that is more perpendicular to the longitudinal direction of the aorta than that given by conventional contrast enhanced-CT, and thus provides a more accurate cross-sectional image of the aneurysm than the latter.

We conclude that, in the experimental phantom study CBCT had a high quantitative reliability, and that, in the clinical study CBCT provided useful information for both qualitatively and quantitatively evaluating AAA before and after stent-grafting. (J Nippon Med Sch 2001; 68: 498—509)

Key words: cone-beam CT, abdominal aortic aneurysm, stents and prostheses, interventional procedure

Introduction

The treatment of abdominal aortic aneurysms (AAA) using stent-grafts (SG), is receiving increasing attention as an alternative to open surgery because of its less invasive nature. The SG procedure consists of taking a bare metal stent and covering it with the fabric used to make vascular prostheses, introducing it from a peripheral artery to the aneurysm via a sheath introducer, and then fixing its upper and lower ends to the normal parts of the aorta, thereby excluding the aneurysmal sac from the blood flow[1,2]. This therapy, to be conducted safely and properly, requires a more exact image of the aneurysm than that required in conventional surgery. Specifically, it is important to understand the shape and size of the aneurysm, its relation with the aortic branches and the caudal extension of the iliac arteries, and then to determine whether or not the aneurysm is suitable for stent-grafting. If the aneurysm is suitable for the stent-grafting, a SG must be designed to accurately fit the given aneurysm[3-14].

An important diagnostic modality for planning this therapy and designing a SG is, at the very least CT and conventional angiography. Of these two, conventional angiography has been regarded as the gold standard for artery imaging. However, an angiogram taken from a single direction does not provide any three-dimensional (3D) information. To three-dimensionally evaluate the vasculature, it would be necessary to add angiograms taken from several other directions as well. In contrast, a rotational digital subtraction angiography (RDSA) system enables us to obtain circumferential projectional images from multiple directions with only a single injection of a contrast medium[15-17]. With this system, however, it is difficult to obtain images from a cranio-caudal direction.

Recently cone-beam computed tomography (CBCT) has been developed, which enables the reconstruction of three-dimensional volume data from multiple projectional data sets obtained by RDSA. With this ability, a 3D image of the vasculature can be assessed from any direction[18-24]. Because CBCT is based on the data sets provided by RDSA, it can be also expected that CBCT has so high a spatial resolution as to allow for an exact quantitative evaluation of the vasculature.

The aim of this study is: 1) to evaluate the quantitativeness of CBCT images in the experimental study, and 2) to evaluate the clinical usefulness of CBCT in the assessment of abdominal aortic aneurysms (AAA) before and after stent-grafting, qualitatively as well as quantitatively.

Materials and Methods

Rotational digital subtraction angiography (RDSA)

For our data acquisition system, a SF-VA 100 system (Hitachi Medical Co., Ltd.,Tokyo, Japan) was used. This system is comprised of an X-ray tube, a high-resolution image intensifier (I.I.) and a TV camera, which are linearly arranged at the two opposite sides of a gantry. The X-ray unit rotates transversely at a rate of 4.8 seconds per a rotation. During rotation, a pulse X-ray exposure is taken at every 1.25 degrees so that 288 images, all with a different view angle, are obtained under computed control. These 288 projectional images are promptly relayed to a monitor display as a series of dynamic rotational images. Digital subtraction images can also be obtained, practically in real time. The display matrix for presenting images comprises 512 × 512 pixels.

Cone-beam CT

To obtain CBCT images, a dedicated workstation DFA-ViR/1 (Hitachi Medical Co., Ltd., Tokyo, Japan) was used. The SF-VA100 produced a series of 2D serial projectional images from 288 different angles before and after injection of a contrast medium, thus totaling 576 framed images, and the images are transmitted, via 10Base-T Ethernet, through a scanner interface to the DFA-ViR/1. The workstation, using preinstalled software for 3D reconstruction based on the Feldkamp algorithm, convert those projectional images into three-dimensional volume data. During this process, in order to eliminate any disturbing effects from the geometrical distortions of the detectors, geomagnetism, and scattered solar rays, the workstation correct these factors using air calibration data sets obtained prior to the study. **Fig. 1** shows an outline of the CBCT imaging system. It is possible to make different 3D images by applying different reconstruction methods to the volume data: when volume rendering (voxel transmission (VT) method) or maximum intensity projection (MIP) are applied, cone-beam 3DCT images (3D-CBCT) or cone-beam MIP images (CB-MIP) are obtained, and further still, conebeam multiplanar reformation/curved planar reformation images (CB-MPR/CPR) can be obtained that allow the reconstruction of any cross-sectional image.

1. *Experimental phantom study*

1) Phantom

Fig. 2 shows a schematic drawing of the phantom used in this study. The phantom was made-to-order (Hitachi Medical Co., Ltd., Tokyo, Japan). An acrylic plate (200 × 134 × 15 mm) was drilled so that four columnar cavities were formed on each side with the median line at the boundary to give eight cavities in total; each columnar cavity served as an imaginary blood vessel. The columnar cavities were termed as A, B, C and D, and A', B', C' and D' as shown in the figure. Cavities A, C and D have a diameter of 10, 5 and 2 mm respectively, while cavity B comprises two cavities, one cavity 10 mm in diameter connected with another cavity 5 mm in diameter. The maximum error for the cross-sectional area of the columnar cavities is ± 0.1 mm, while the maximum error along the longitudinal axis is ± 0.2 mm. This acrylic plate was designed to be placed in a cylinder 165 mm in diameter × 280 mm in length. The eight cavities serving as phantom vessels were filled with 300 mgI/m*l* of a non-ionic iodinated monomer contrast medium (Iopromide, Tanabe Seiyaku, Osaka, Japan). The space surrounding the acrylic plate was filled with water deprived of air. The phantom was placed at the center of the I.I. The images of the phantom were obtained under the following parameters: X-ray tube voltage at 77 kV with a 12 inch I.I., X-ray tube current at 400 mA, the pulse width at 2 ms, and the scan time at 4.8 sec/rotation.

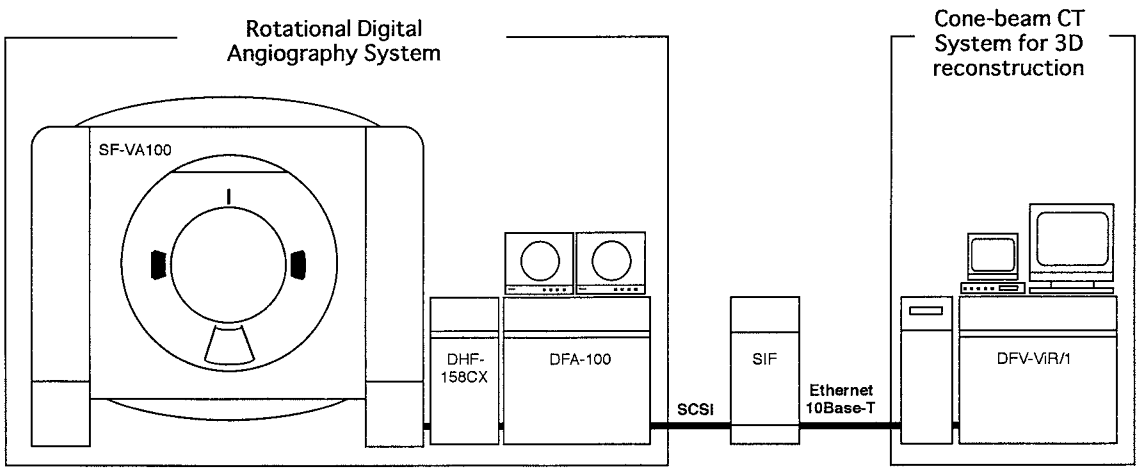

Fig. 1 An outline of the imaging system.

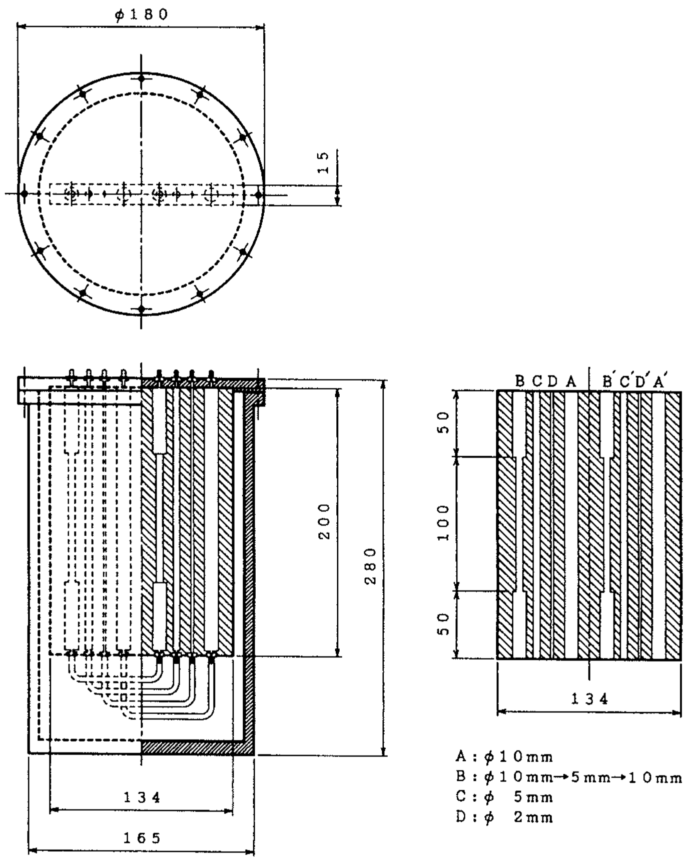

Fig. 2 A schematic drawing of the experimental phantom.

2) Evaluation of the images

For the quantitative analysis of the phantom, CB-MPR/CPR images were used. The images of the eight columnar cavities sectioned at the plane passing through their longitudinal axes were reconstructed, two lines P-Q and R-S were drawn across the images of eight cavities, the distance between two paired intersections of each cavity were manually measured, and the distance was taken as the diameter of that cavity (**Fig. 3**).

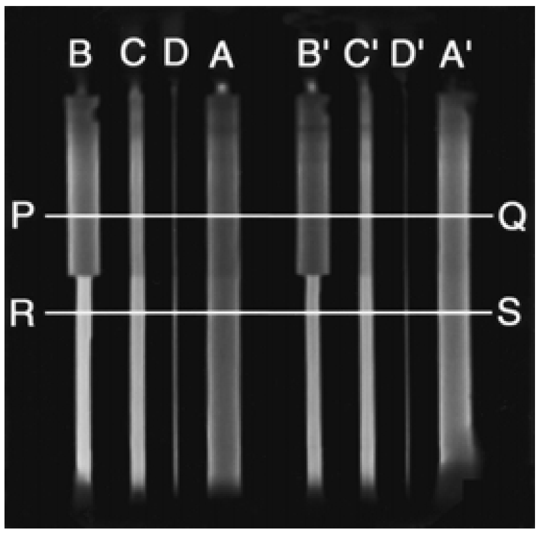

Fig. 3 For the image of each columnar cavity, the intersections of the cavity surface with lines P-Q and R-S were determined, and the intervals between the paired intersections were measured with a scale.

3) Measurements

For each cavity image obtained by CB-MPR/CPR, two radiologists (K. I. and H.H.) independently measured the diameter at two sites, and each of them repeated the same measurement ten times (for a total of 160 measurements for each radiologist). For each cavity, the measurements from the two radiologists were summed to give an average; and this was made the final average measurement for the cavity. The result was calculated to a decimal place. The statistical analysis was performed as follows: the averaged diameter of each cavity was compared using the paired t-test with the actually determined diameter of the same cavity obtained during preparation of the phantom and a difference was judged to be significant at p<0.05.

2. *Clinical Evaluation*

1) Patients

Out of 18 consecutive patients who had been diagnosed with infrarenal AAA by diagnostic imaging other than RDSA, and who subsequently received RDSA to determine whether their aneurysms were suitable for SG, from July 1997 to June 2000, nine patients, who met the criteria for the stent-grafting, and who underwent conventional contrast enhanced-CT and angiography before and after surgery, were selected (**Table 1**). The patients were all male (an average of 68 years old: 56～80). The other nine patients were excluded from the study because seven were found not to be suitable for the stent-grafting (five showed markedly tortuous aneurysms including their necks, and two the extremely tortuous course of the iliac arteries) and two, although they received SG, did not have any CT or angiographic images taken after the stent-grafting.

2) Angiographic examination with RDSA

To perform RDSA on the abdominal aorta, a 12-inch I.I. was used throughout the study. The contrast medium consisted of a non-ionic iodinated monomer solution with a concentration of 300 mgI/m*l* (Iopromide, Tanabe Seiyaku, Osaka, Japan, and, Iohexol, Daiichi Pharmaceutical Co., LTD., Tokyo, Japan). A pigtail catheter with a 5 Fr. diameter (Medikit Co., Ltd., Tokyo, Japan), which has a tip with X-ray opaque dotts inscribed at 1 cm intervals, was used. The catheter tip was settled in the abdominal aorta at an interval between the origins of the celiac artery and the superior mesenteric artery, and the contrast medium was injected at a rate of 15～20 m*l*/sec for a total dosage of 25～45 m*l*. RDSA images were obtained under the following parameters: tube voltage at 75～80 kV, tube current at 400～500 mA, pulse width at 4 msec, and scan time at 4.8 sec/rotation.

Table 1 Summary of cases

Case	Age	Sex	Aneurysm		Stent-Graft
			Shape	Level	
1	80	M	fusiform	infra-renal	bifurcated
2	78	M	fusiform	infra-renal	bifurcated
3	74	M	fusiform	infra-renal	bifurcated
4	73	M	saccular	infra-renal	straight
5	71	M	fusiform	infra-renal	bifurcated
6	67	M	fusiform	infra-renal	bifurcated
7	64	M	fusiform	infra-renal	straight
8	57	M	saccular	infra-renal	straight
9	54	M	saccular	infra-renal	straight

3) Stent-graft Implantation

Stent-graft implantation was performed only in patients who had been informed about the procedure and the possible complications in detail. The ethics committee of our institute approved the study protocol. The surgery was performed in the angiography suite on all of the patients with the cooperation of a radiologist, a cardiovascular surgeon and an anesthesiologist. Under intravenous or general anesthesia, a femoral artery was opened and a SG was inserted, under fluoroscopy, via a long sheath introducer, 16～20 Fr. in diameter. The SGs were all hand-made: the bare stent had an original-Z or spiral-Z structure made of stainless steel, and it was covered by a polyester fabric used for vascular prostheses. After the procedure, each patient stayed in an intensive care unit for 24 hours so that his post-operative hemodynamics could be observed. After their hemodynamics stabilized, the patient was transferred to a general ward.

4) Clinical evaluations

(1) Pre-operative evaluation

The qualitative evaluation using a 3D-CBCT image was carried out based on (A-1) the shape of an aneurysm, and (A-2) the anatomical relationship between the aneurysm and aortic branches, and (A-3) the caudal extension of the aneurysm towards the iliac arteries. The 3D-CBCT images were obtained, following the manufacturer's specifications, with the threshold set at 0～3,000 and the opacity at 1.4. The 3D-CBCT images were visually compared with angiographic images of the same artery obtained by RDSA. For each evaluation, when one (X) was more excellent than the other (Y), the evaluation was expressed as X>Y; when X was equal to Y, the evaluation was expressed as X=Y.

The qualitative analysis of AAA using a CB-MPR/

CPR image was carried out based on: (B-1) the inflection angle of the aneurysm; (B-2) the diameter of the aneurysm; (B-3) the diameter of the proximal and distal neck; and (B-4) the distance of the proximal and distal neck. The proximal neck is the proximal end of the aneurysm to the origin of the renal artery, and the distal neck is from the distal end of the aneurysm to the aortic bifurcation. For items (B-1) and (B-4), the measurements were compared with the corresponding results obtained by conventional angiography. For items (B-2) and (B-3), The measurements were performed using a section perpendicular to the longitudinal axis of the aorta, and were then compared with the results based on the contrast-enhanced CT images with a slice thickness of 5 mm.

(2) Post-operative evaluation

The qualitative analysis of AAA using CB-MIP images was carried out based on (C-1) the visibility of the stent, (C-2) the migration of the stent, (C-3) the deformation of the stent, and (C-4) the endoleak. For item (C-1), a CB-MIP image, which was able to most finely recognize the structure of the stent, was ranked as "excellent", and the other images were classified as either "good", "fair", or "poor", according to their ability to visualize the stent. For items (C-2) and (C-3), the results were compared with those obtained from plain radiographs taken after stent-grafting. For item (C-4), a sectional image reconstructed by CB-MPR/CPR along the longitudinal axis of the aorta was used, and compared with the results from CT images.

The qualitative analysis after stent-grafting was independently performed by two radiologists (K.I., and H.H.), and they then discussed their assessment with each other to determine its final grade.

The quantitative analysis after stent-grafting was carried out as follows. For each image, the two radiologists measured two times independently. Then the measurements were summed to give an average, and this was made the final average of the measurements. The result was calculated to a decimal place. The statistical analysis was made as follows: the average of each parameter obtained from a CBCT image was compared with the corresponding results using the paired t-test and a difference was judged to be significant at $p<0.05$.

Results

1. *Experimental phantom study*

Table 2 lists the results of the measurements based on the CB-MPR/CPR images. For all of the cavities tested, there was no significant difference between

Table 2 Results of the experimental phantom study

P − Q	B	C	D	A
True value of diameter (mm)	10	5	2	10
mean ± S.E. (mm) paired T-test	10.05 ± 0.04 N.S.	4.99 ± 0.03 N.S.	1.98 ± 0.04 N.S.	9.95 ± 0.04 N.S.
	B′	C′	D′	A′
True value of diameter (mm)	10	5	2	10
mean ± S.E. (mm) paired T-test	9.97 ± 0.05 N.S.	4.98 ± 0.04 N.S.	2.01 ± 0.03 N.S.	9.99 ± 0.04 N.S.

R − S	B	C	D	A
True value of diameter (mm)	5	5	2	10
mean ± S.E. (mm) paired T-test	5.03 ± 0.03 N.S.	5.03 ± 0.04 N.S.	1.98 ± 0.04 N.S.	9.98 ± 0.05 N.S.
	B′	C′	D′	A′
True value of diameter (mm)	5	5	2	10
mean ± S.E. (mm) paired T-test	4.98 ± 0.03 N.S.	4.97 ± 0.03 N.S.	1.98 ± 0.04 N.S.	9.99 ± 0.04 N.S.

Table 3　Clinical comparison of 3D-CBCT and RDSA

Case	A-1	A-2	A-3
	Shape of AAA	Relationship between the AAA and the aortic branches	Involvement with the CIA
1	3D-CBCT ＞ RDSA	3D-CBCT ＜ RDSA	Not available
2	3D-CBCT ＞ RDSA	3D-CBCT ＞ RDSA	3D-CBCT ＝ RDSA
3	3D-CBCT ＝ RDSA	3D-CBCT ＞ RDSA	3D-CBCT ＝ RDSA
4	3D-CBCT ＝ RDSA	3D-CBCT ＝ RDSA	3D-CBCT ＝ RDSA
5	3D-CBCT ＞ RDSA	3D-CBCT ＞ RDSA	3D-CBCT ＝ RDSA
6	3D-CBCT ＝ RDSA	3D-CBCT ＞ RDSA	3D-CBCT ＞ RDSA
7	3D-CBCT ＞ RDSA	3D-CBCT ＞ RDSA	3D-CBCT ＝ RDSA
8	3D-CBCT ＞ RDSA	3D-CBCT ＞ RDSA	3D-CBCT ＞ RDSA
9	3D-CBCT ＝ RDSA	3D-CBCT ＜ RDSA	3D-CBCT ＝ RDSA

3D-CBCT : 3-dimensional cone-beam computed tomography, AAA : abdominal aortic aneurysm, CIA : common iliac artery, RDSA : rotational digital subtraction angiography

Fig. 4　A 3D-CBCT image (left posterior oblique with 85 degrees) taken from a patient with saccular AAA (case 8). An AAA is clearly demonstrated. The main branches such as the renal arteries, the superior and inferior mesenteric arteries, and the iliac arteries are also clearly depicted.

the average of the measurements based on the CB-MPR/CPR images and the measurements actually performed on the phantom itself.

2. *Clinical evaluation*

1) The qualitative evaluation before stent-grafting (Table 3, Fig. 4)

(A-1) the shape of an aneurysm. 3D-CBCT was equally or more highly evaluated than RDSA in all of the patients, because it enabled viewing of the aneurysm from an optimal angle, including cranio-caudal directions, in contrast with the latter. (A-2) the anatomical relationship between the aneurysm and the aortic branches. 3D-CBCT was evaluated more highly than, or as highly as RDSA in seven patients out of nine. For the other two patients, RDSA was judged to more clearly demonstrate the vasculature, especially of the renal arteries. (A-3) the caudal extension of the aneurysm towards any of the iliac arteries. One patient did not yield any relevant data, and, of the remaining eight patients, four showed positive findings suggestive of the involvement to an iliac artery on the 3D-CBCT images, while the other four showed no involvement. For six of these eight patients, the 3D-CBCT results were judged equal to the RDSA results. For the other two patients, the 3D-CBCT results were judged superior to the RDSA results.

2) Quantitative evaluation before stent-grafting (Table 4, Figs. 5, 6, and 7a to 7c)

As regards the inflection angle of the aneurysm (B-1) and the distance of the proximal and distal neck (B-3), the results from CB-MPR/CPR images were not significantly different from those obtained by conventional angiography. However, concerning the diameter of the aneurysm (B-2), and the diameter of the proximal and distal neck (B-4), the measurements obtained from the CT images were significantly larger than those obtained by CB-MPR/CPR ($p<0.05$).

Table 4 Clinical comparison of CBCT and other modalities, regarding the measurements

Case	B-1		B-2		B-3				B-4			
	Angle of AAA (degree)		Diameter of AAA (mm)		Distance of PN (mm)		Distance of DN (mm)		Diameter of PN (mm)		Diameter of DN (mm)	
	CB-MPR/CPR	AG	CB-MPR/CPR	CT	CB-MPR/CPR	AG	CB-MPR/CPR	AG	CB-MPR/CPR	CT	CB-MPR/CPR	CT
1	134.6	137.2	45.0	45.8	68.3	67.2	3.3	3.1	18.5	20.0	21.6	22.0
2	152.5	157.3	30.3	31.2	30.9	32.0	0.0	0.0	20.4	21.2	0.0	0.0
3	106.2	108.6	31.7	31.6	48.4	50.2	0.0	0.0	17.9	18.1	0.0	0.0
4	165.0	170.5	19.9	20.2	51.2	52.1	15.4	15.2	16.8	18.0	17.2	18.0
5	126.2	120.2	34.6	34.8	22.3	22.2	0.0	0.0	15.6	16.7	0.0	0.0
6	157.4	158.4	34.6	34.9	25.0	25.2	0.0	0.0	18.5	19.0	0.0	0.0
7	147.2	145.5	30.9	31.5	51.3	53.3	4.3	4.1	16.0	16.5	16.8	17.2
8	166.4	170.2	19.1	20.3	5.8	5.2	61.2	55.6	11.2	12.4	13.8	14.2
9	162.5	160.2	28.4	28.6	25.8	57.5	18.9	21.4	15.8	16.0	13.5	14.5
mean ± S.E.	146.4 ± 6.8	147.6 ± 7.3	30.5 ± 2.6	31.0 ± 2.6	36.6 ± 6.5	40.5 ± 6.8	11.5 ± 6.7	11.0 ± 6.1	16.7 ± 0.9	17.5 ± 0.9	9.2 ± 3.0	9.5 ± 3.1
paired T-test	N.S.		$p < 0.05$		N.S.		N.S.		$p < 0.05$		$p < 0.05$	

AAA : abdominal aortic aneurysm, AG : angiography, CT : computed tomography, CB-MPR/CPR : cone-beam multiplanar reformation/curved planar reformation, DN : distal neck, PN : proximal neck

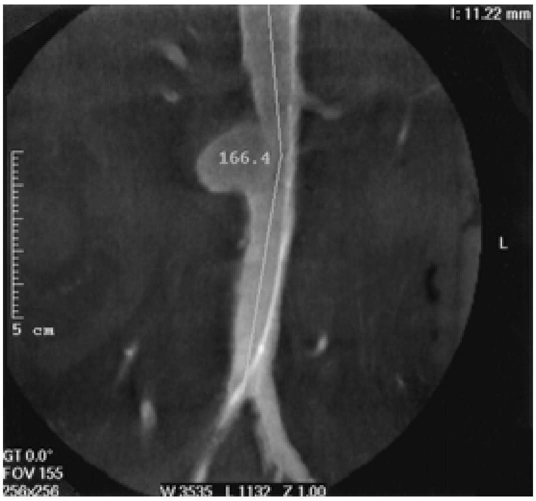

Fig. 5 A CB-MPR/CPR image used to measure the inflection angle of an aneurysm (from case 8). The angle is measured as 166.4 degrees.

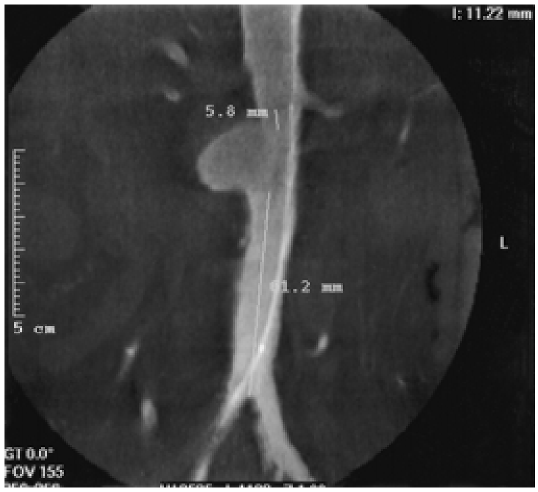

Fig. 6 CB-MPR/CPR images enables measuring the distance of the proximal and distal neck. Each distance is measured as 5.8 and 61.2 mm, respectively.

3) Quantitative evaluation after stent-grafting (Table 5, Figs. 8a and 8b)

[1] As regards the visibility of the stent using CB-MIP images, three patients were ranked as excellent, two as good, three as fair and one as poor. [2] Concerning the detectability of the stent migration (C-2), and the stent deformation (C-3), the results from the CB-MIP images yielded the same assessment as those from plain radiographs. [3] Concerning endoleak detectability, the results from the CB-MPR/CPR images yielded the same assessment as those from CT. No endoleaks were detected in any of the patients.

Discussion

Stent-graft implantation as a new treatment for AAA was first reported by Parodi et al. in 1991, and has recently attracted attention because of its less invasive nature compared with conventional open surgery[1,2]. However, an AAA specific SG is not commercially available in Japan. Therefore, in the majority of hospitals in Japan, an operator must design and make a SG suitable for each patient by himself[12]. To design a SG suitable for each patient and to determine the proper location to anchor the SG, it is important to know in advance a number of facts about

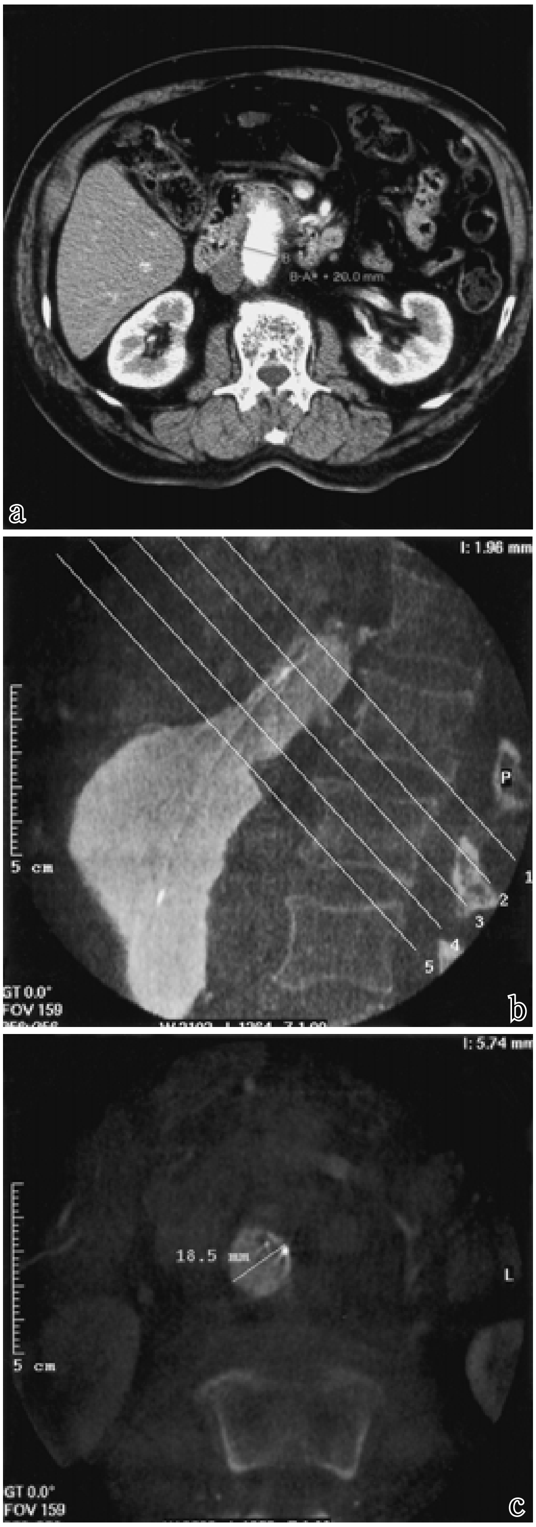

Fig. 7 Measuring the diameter of the proximal neck using CT and CB-MPR/CPR images (case 8).
a. An axial contrast-enhanced CT image of the same case. The diameter of the proximal neck is measured as 20 mm.
b. A scout image of CB-MPR/CPR, cutting along the longitudinal direction of the aorta.
c. An axial image of CB-MPR/CPR obtained from position number 3 on the scout image. The diameter of the proximal neck is measured as 18.5 mm.

the aneurysm. This information is usually elucidated through CT and conventional angiography and includes, from a qualitative aspect, the shape of the aneurysm, the caudal extension towards the iliac arteries, the anatomical relation to the aortic branches (mainly with the renal arteries), and their patency. Also included, from a quantitative aspect, is the inflection angle of the aneurysm, the diameter of the proximal and distal neck, and the distances of the two necks, which will serve as a landing zone[3-14]. However, CT does not always give an accurate sectional image that is perpendicular to the longitudinal direction of the aorta, and furthermore, the cranio-caudal extension of the aneurysm is difficult to determine by axial CT images. Conventional angiography, as a standard in the diagnosis of AAA, gives only a projected image, and does not always enable evaluation of the aneurysm from an optimal viewing angle.

In contrast, RDSA provides projectional images arranged from 288 directions with just one injection of contrast medium, and thus enables evaluation of the aneurysm from an optimal viewing angle. However, with this method it is difficult to obtain an image from a cranio-caudal direction[15-17]. Recently, to overcome these limitations, CBCT was developed. This method consists of processing data sets obtained by RDSA using the Feldkamp algorithm, in order to convert them into 3D volume data[18,20,22,25]. CBCT can reconstruct three different kinds of images; that is, 3D-CBCT, CB-MIP and CB-MPR/CPR. With a 12-inch I.I. and a matrix of 256 pixels for 3D reconstruction, the theoretical spatial resolution is $0.8 \times 0.8 \times 0.8$ mm, and thus obtaining a high-quantity 3D image consisting of an isotropic voxel can be expected[18,20,22]. However, it is known that when using the Feldkamp algorithm the margins of I.I. will be slightly deformed. To evaluate this disturbing effect, we carried out quantitative analysis of CBCT images using the experimental phantom[25,26]. As long as the measurement was restricted within a central area of I.I., there were no statistically significant differences between the results from the CBCT images and from the actual measurement. On the basis of this result, we concluded that the CBCT images are reliable enough for designing a SG, a process that requires an accurate measurement. 3D-CBCT provides 3D static or motion images, and enables

Table 5 Clinical comparison of CBCT and other modalities, regarding the visibility of the stent, and the detectability of the endoleak

Case	C-1	C-2		C-3		C-4	
	Visibility of SG	Migration of SG		Deformation of SG		Leakage	
	CB-MIP	CB-MIP	Radiogram	CB-MIP	Radiogram	CB-MPR/CPR	CT
1	poor	(−)	(−)	(+)	(+)	(−)	(−)
2	good	(−)	(−)	(−)	(−)	(−)	(−)
3	fair	(−)	(−)	(−)	(−)	(−)	(−)
4	good	(−)	(−)	(−)	(−)	(−)	(−)
5	excellent	(−)	(−)	(+)	(+)	(−)	(−)
6	excellent	(−)	(−)	(−)	(−)	(−)	(−)
7	fair	(−)	(−)	(−)	(−)	(−)	(−)
8	fair	(−)	(−)	(−)	(−)	(−)	(−)
9	excellent	(−)	(−)	(+)	(+)	(−)	(−)

3D-CBCT : 3-dimensional cone-beam computed tomography, MIP : maximum intensity projection, MPR/CPR : multiplanar reformation/curved planar reformation, SG : stent-graft

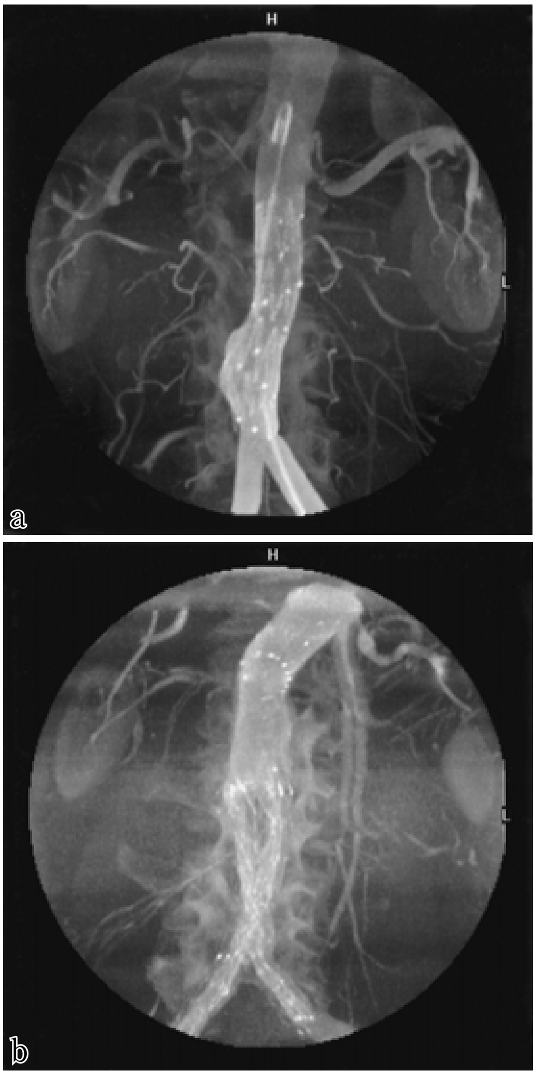

Fig. 8 Qualitative assessment of AAA after stent-grafting using CB-MIP images.
a. A case of saccular AAA treated with a straight SG judged "excellent". The structure of the stent is clearly identified.
b. A case of saccular AAA treated with a bifurcated SG judged "poor" because of patient's difficulty in holding his breath under venous anesthesia.

evaluation of the vasculature from an optimal direction, which is almost impossible with conventional angiography. Moreover, because this method enables us to understand the anatomical relationship between the aneurysm and the aortic branches, it is helpful not only for designing the SG but also for determining the proper location to anchor the SG. Although the CB-MIP technique provides only projectional images, and will not allow a 3D view of the vasculature, it represents the accurate X-ray absorption of the object, and is the most useful in the assessment of the migration or deformation of a stent. The CB-MPR/CPR technique allows the optimal sectional image of the vasculature to be obtained even including curved sections along the longitudinal direction of the aorta. Therefore, with this technique, it is easy to determine the distance or angle between two arbitrarily chosen points in the image. The inflection angle of the aneurysm, and the distance of the proximal and distal necks obtained by CB-MPR/CPR were compared with those obtained by conventional angiography, and there were no significant differences between the two modalities. From these results, we concluded that CB-MPR/CPR could be useful for designing the SG, and for determining the proper location to anchor the SG. As regards the diameter of the aneurysm, and the diameter of the proximal and distal neck, the results from CB-MPR/CPR images were significantly different from those based on conventional contrast enhanced-CT images. This is probably because a CT scan only provides the sectional image cut perpendicularly to the longitudinal axis of the patient, ignoring the tortuosity and inflection of the aorta, whereas CB-MPR / CPR provides the sectional image rightly perpendicular to the longitudinal direction of the aorta. In view of this, we considered that CBCT images would be superior to conventional contrast enhanced-CT images in allowing a more accurate determination of the diameter of an aneurysm.

However, this study also revealed some limitations inherent to a CBCT system.

For item (A-2), 3D-CBCT was inferior to RDSA in two patients. In those two patients, the bilateral renal arteries were clearly demonstrated on the RDSA images while they were poorly depicted on the 3D-CBCT images. The reason is ascribed to the fact that an image was taken at a time best suited for obtaining an optimal view of the aneurysm itself, and that the 3D-CBCT's threshold was set for the optimal image for demonstrating the aneurysm. Indeed, when the threshold range was widened to cover small arteries, it was possible to obtain a clearer image of the renal arteries. Moreover, as regards item (A-3), 3D-CBCT was inferior to RDSA in one case. This is because, although RDSA includes the common iliac arteries in its visual field and thus gives an optimal view of them, 3D-CBCT cannot include them in its visual field. This phenomenon is the result of the truncation which was executed automatically by the algorithm when reconstructing the volume data, in order to dispose of data at the margins of the visual field because of their low reliability[27]. However, it is possible to avoid such truncation effects by setting the object on a central area of I.I. with sufficiently wide margins. As regards the mural thrombus of an aneurysm, CBCT could not detect it in the study. This is probably because RDSA is based on the use of an I. I., which lowers the contrast resolution. It is expected that a new model incorporating a flat panel detector that has a high contrast resolution will solve this problem in the near future[28–30]. For item (C-4), no endoleaks were detected in any of the patients either in CB-MPR/CPR or CT images. However, an endoleak so small as not to sufficiently reach the contrast media in such a short scan time as 4.8 sec might go undetected, especially by CBCT. To eliminate this possibility a further study will be necessary, both for CB-MPR/CPR and CT.

In conclusion, we consider that in the experimental phantom study CBCT has a high quantitative reliability, and that in the clinical study CBCT provides more useful information for qualitative and quantitative evaluation of AAA before and after stent grafting.

References

1. Parodi JC, Palmaz JC, Barone HD: Transfemoral intraluminal graft implantation for abdominal aortic aneurysm. Ann Vasc Surg 1991; 5: 491–499.
2. Blum U, Voshage G, Lammer J, Beyersdorf F, Töllner D, Kretschmer G, Spillner G, Polterauer P, Nagel G, Hölzenbein T, Thurnher S, Langer M: Endoluminal stent-grafts for infrarenal abdominal aortic aneurysms. N Engl J Med 1997; 336: 13–20.
3. Armon MP, Whitaker SC: Preoperative assessment of aneurysm. Operative Atlas of Endoluminal Aneurysm Surgery, Yusuf SW, Marin ML, Ivancev K, Hopkinson BR eds. 2000; pp 3–22, ISIS MEDICAL MEDIA LTD, Oxford.
4. Gomes MN, Davros WJ, Zeman RK: Preoperative assessment of abdominal aortic aneurysm: the value of helical and three-dimensional computed tomography. J Vasc Surg 1994; 20: 367–375.
5. Dorffner R, Thurnher SA, Youssefzadeh S, Winkelbauer F, Hölzenbein T, Polterauer P, Lammer J: Spiral CT angiography in the assessment of abdominal aortic aneurysms after stent grafting: value of maximum intensity projections. J Comput Assist Tomogr 1997; 21: 472–477.
6. Nawaratne S, Fabiny R, Brien JE, Zalcberg J, Cosolo W, Whan A, Morgan DJ: Accuracy of volume measurement using helical CT. J Comput Assist Tomogr 1997; 21: 481–486.
7. Thurnher SA, Dorffner R, Thurnher MM, Winkelbauer FW, Kretschmer G, Polterauer P, Lammer J: Evaluation of abdominal aortic aneurysm for stent-graft placement: comparison of gadolinium-enhanced MR angiography versus helical CT angiography and digital subtraction angiography. Radiology 1997; 205: 341–352.
8. Berg MH, Manninen HI, Vanninen RL, Vainio PA, Soimakallio S: Assessment of renal artery stenosis with CT angiography: usefulness of multiplanar reforma-

tion, quantitative stenosis measurements, and densitometoric analysis of renal parenchymal enhancement as adjuncts to MIP film reading. J Comput Assist Tomogr 1998; 22: 533–540.
9. Moritz JD, Rotermund S, Keating DP, Oestmann JW: Infrarenal abdominal aneurysms: implications of CT evaluation of size and configuration for placement of endovascular aortic stent grafts. 1998; Radiology 198: 463–466.
10. Rubin GD, Paik DS, Johnston PC, Napel S: Measurement of the aorta and its branches with helical CT. Radiology 1998; 206: 823–829.
11. Armerding MD, Rubin GD, Beaulieu CF, Slonim SM, Olcott EW, Samuels SL, Jorgensen MJ, Semba CP, Jeffray RB Jr, Dake MD: Aortic aneurysmal disease: assessment of stent-graft treatment-CT versus conventional angiography. Radiology 2000; 215: 138–146.
12. Ishiguchi T, Ohta T, Takai K: Imaging for evaluation and measurement of aortic aneurysm for endovascular stent-grafting. Japanese Journal of Diagnostic Imaging 2000; 20: 859–866.(in Japanese)
13. Zempo N, Esato K: Image diagnosis of aortic aneurysm: surgeon's expectation of the radiologist. Japanese Journal of Diagnostic Imaging 2000; 20: 878–879. (in Japanese)
14. Ishiguchi T: Aortic imaging for endovascular stent-grafting: evaluation with helical CT and MR angiography. Japanese Journal of Interventional Radiology 2000; 15: 319–323.(in Japanese)
15. Kumazaki T: Development of a new digital angiography system: improvement of rotational angiography and three-dimensional image display. Nippon Acta Radiologica 1991; 51: 1068–1077.(abst. in English)
16. Kumazaki T: Rotational stereo-digital radiography: theoretical model of new 3-D angiography display and development of a new system. J Nippon Med Sch 1992; 59: 441–449.(in Japanese)
17. Kumazaki T: Rotational digital angiography. Japanese Journal of Diagnostic Imaging 1997; 17: 64–72. (in Japanese)
18. Kumazaki T: Cone-beam 3D-CT-3D-CT image reconstructed from the rotational digital subtraction angiography system-. New Horizons of 3D-CT Imaging—Current Concepts and Applications—, Kumazaki T, Kobayashi H, eds. 1995; pp 17–23, Nankodo Co., Ltd., Tokyo.(in Japanese)
19. Kobayashi H: Basic principle of voxel transmission method. New Horizons of 3D-CT Imaging—Current Concepts and Applications—, Kumazaki T, Kobayashi H, eds. 1995; pp 2–11, Nankodo Co., Ltd., Tokyo. (in Japanese)
20. Kumazaki T: Cone-beam 3D-CT. Jpn J Clin Radiol 1996; 41: 1401–1408.(in Japanese)
21. Genma K, Kumazaki T: Clinical usefulness of rotational stereo-digital angiography for the diagnosis of aortic dissection. J Jap Coll Angiol 1992; 32: 297–307. (abst. in English)
22. Ichikawa K, Hayashi H, Kumazaki T: Three-dimensional imaging of the vasculature—development of rotational digital angiography and cone-beam CT system—. J Jpn Soc Biorheol 1998; 12: 148–156. (in Japanese)
23. Ichikawa K, Takagi R, Hayashi H, Kawamata H, Kumazaki T, Yoshida Y, Node Y, Teramoto A: A case of giant aneurysm of internal carotid artery; clinical usefulness of cone-beam 3D-CT images. Jpn J Clin Radiol 1998; 43: 621–624.(abst. in English)
24. Ichikawa K, Kumazaki T, Hayashi H, Tajima H, Kawamata H, Goto S, Takahashi S, Okajima Y: A preliminary clinical assessment of image intensifier (I.I.)-based cone-beam 3D-CT for the evaluation of vascular lesions. J Jap Coll Angiol 1999; 39: 93–97. (abst. in English)
25. Feldkamp LA, Davis LC, Kress JW: Practical conebeam algorithm. J Opt Soc Am 1989; [A] 1: 612–619.
26. Ning R, Kruger RA: Image intensifier-based computed tomography volume scanner for angiography. Acad Radiol 1996; 3: 344–350.
27. Cho PS, Rudd AD, Johnson RH: Cone-beam CT from width-truncated projections. Computerized Medical Imaging & Graphics 1996; 20: 49–57.
28. Siewerdsen JH, Jaffray DA: Cone-beam computed tomography with a flat-panel imager: effects of image lag. Medical Physics 1999; 26: 2635–2647.
29. Spahn M, Strotzer M, Volk M, Bohm S, Geiger B, Hahm G, Feuerbach S: Digital radiography with a large-area, amorphous-silicon, flat-panel X-ray detector system. Radiology 2000; 35: 260–266.
30. Garmer M, Hennigs SP, Jager HJ, Schrick F, van de Loo T, Jacobs A, Hanusch A, Christmann A, Mathias K:Digital radiography versus conventional radiography in chest imaging: diagnostic performance of a large-area silicon flat-panel detector in a clinical CT-controlled study. AJR 2000; 174: 75–80.

(Received, April 18, 2001)
(Accepted, June 5, 2001)